Earth Surf. Dynam., 2, 279–293, 2014
www.earth-surf-dynam.net/2/279/2014/
doi:10.5194/esurf-2-279-2014

Earth Surface Dynamics
Open Access

Morphodynamic regime change in a reconstructed lowland stream

J. P. C. Eekhout[1], **R. G. A. Fraaije**[2], **and A. J. F. Hoitink**[1]

[1]Hydrology and Quantitative Water Management Group, Wageningen University, Wageningen, the Netherlands
[2]Ecology and Biodiversity Group, Institute of Environmental Biology, Utrecht University, Utrecht, the Netherlands

Correspondence to: J. P. C. Eekhout (joriseekhout@gmail.com)

Received: 15 October 2013 – Published in Earth Surf. Dynam. Discuss.: 15 November 2013
Revised: 15 April 2014 – Accepted: 23 April 2014 – Published: 26 May 2014

Abstract. With the aim to establish and understand morphological changes in response to channel reconstruction, a detailed monitoring plan was implemented in a lowland stream called Lunterse Beek, located in the Netherlands. Over a period of almost 2 years, the monitoring programme included serial morphological surveys, continuous discharge and water level measurements, and riparian vegetation mapping, from photographs and field surveys. Morphological processes occurred mainly in the initial period, before riparian vegetation developed. The initial period was largely dominated by upstream sediment supply, which was associated with channel incision upstream from the study area. Herbaceous vegetation started to develop approximately 7 months after channel reconstruction. The monitoring period included two growing seasons. A clear increase of riparian vegetation cover from first to the second year was observed. Detailed morphological and hydrological data show a marked difference in morphological behaviour between the pre-vegetation and post-vegetation stage. A linear regression procedure was applied to relate morphological activity to time-averaged Shields stress. In the initial stage after channel reconstruction, with negligible riparian vegetation, channel morphology adjusted, showing only a weak response to the discharge hydrograph. In the subsequent period, morphological activity in the channel showed a clear relation with discharge variation. The two stages of morphological response to the restoration measures may be largely associated with the upstream sediment supply in the initial period. Riparian vegetation may have played a substantial role in stabilizing the channel banks and floodplain area, gradually restricting the morphological adjustments to the channel bed.

1 Introduction

Stream restoration in the Netherlands increasingly involves the development of riparian zones along reconstructed channel reaches. These riparian zones are constructed with the aim to accommodate water during flood events and to improve the connection between aquatic and terrestrial ecology. The current contribution describes the initial morphological, hydrological and ecological developments of a reconstructed lowland stream, focussing on the controls of upstream sediment supply and riparian vegetation on the initial morphologic developments after channel reconstruction.

A stream is considered to be in morphological equilibrium when, over a period of years, the channel slope is delicately adjusted to provide, with available discharge and the prevailing channel characteristics, enough flow velocity required for transportation of all of the sediment load supplied from upstream (Mackin, 1948). Leopold and Bull (1979) extended Mackin's definition with more dependent variables, including channel depth, channel width, bed roughness and planform pattern. The dependent variables describe the morphological regime resulting from the coupled system of flow, sediment transport and bed morphology, which may be developing towards a new equilibrium. In this theoretical framework, a local stream restoration effort can be seen as a local perturbation of the morphodynamic system that may trigger a regime change.

After completion of a lowland restoration project, there are two factors particularly relevant in the morphological adjustments towards a new equilibrium, viz. conditions at the boundaries and riparian vegetation development. Typically, stream restoration is applied to isolated sections of a stream, which may cause a compatibility mismatch at the boundaries of the reconstructed stream section. Longitudinal bed level profile adjustments are often initiated at these boundaries, where gradients in flow velocity and sediment transport cause erosion or deposition of the bed. In agricultural areas, such as those presented in this study, weirs located upstream often act as a sediment trap, resulting in supply-limited conditions at the upstream boundary of the reconstructed stream section. At the downstream boundary of the reconstructed stream, backwater effects may cause deceleration of the flow, resulting in deposition and flattening of the bed level slope (Eekhout et al., 2013).

The role of riparian vegetation in channel morphodynamics has been widely recognized, which is highly relevant in the context of stream restoration. Root-reinforced soils are more resistant to deformation and failure than bare soils (Abernethy and Rutherfurd, 2001), which may contribute to bank stability in reconstructed streams (e.g. Simon and Collison, 2002; Pollen-Bankhead and Simon, 2009). Hydrological processes induced by riparian vegetation may decrease bank stability, acting to control infiltration through macropores and the associated pore-water pressure variation (Simon and Collison, 2002). Laboratory experiments have shown how riparian vegetation may stabilize floodplain material, causing initial braided channel patterns to shift towards single-thread meandering channels (Gran and Paola, 2001; Tal and Paola, 2007; Braudrick et al., 2009; Tal and Paola, 2010). Model studies have shown that riparian vegetation is potentially responsible for changes in meander planform characteristics (Perucca et al., 2007). Riparian vegetation density and root structure have shown to be the most influential parameters controlling reach scale morphodynamics (Van de Wiel and Darby, 2004), which in turn may govern the morphological development towards a new equilibrium in a reconstructed stream.

Serial digital elevation models (DEMs) offer the opportunity to quantify reach-scale morphological change. Several survey techniques have been used to collect topographic data for DEM construction in fluvial environments, including total station (Fuller et al., 2003), ground-based GPS (Brasington et al., 2003), photogrammetry (Lane et al., 2010), unmanned radio-controlled platforms (Lejot et al., 2007), terrestrial laser scanning (TLS; Wheaton et al., 2013) and airborne lidar (Croke et al., 2013). Temporal morphological changes could be detected when a study reach is surveyed more than once. A DEM of difference (DoD) may quantify morphological changes when comparing two serial DEMs (Lane et al., 2003). DoDs in braided rivers have been extensively applied on a reach scale (e.g. Lane et al., 2010; Wheaton et al., 2010b, 2013), whereas DoD analysis in meandering rivers is often restricted to a bend scale (e.g. Gautier et al., 2010; Kasvi et al., 2013), although there are several exceptions (Fuller et al., 2003; Erwin et al., 2012; Croke et al., 2013). Until now, DoD analyses have been typically based on annual (e.g. Wheaton et al., 2013) or biannual surveys (Fuller et al., 2003; Lane et al., 2010). The low temporal resolution can cause erosional and depositional patches to overlap, complicating sediment budget estimation. In addition to sediment budget estimation, DoD analysis has been used to relate individual erosional or depositional patches to morphological and ecological processes (e.g. Grove et al., 2013; Wheaton et al., 2010a), which renders it a valuable tool for morphology monitoring after stream reconstruction.

In the context of stream restoration and beyond, there is a need for reach-scale field studies on the interaction between morphology and riparian vegetation (Camporeale et al., 2013). Here, a field study is presented based on 14 high-resolution morphological surveys over a period of almost 2 years, which places this study among the highest temporal resolution DoD analyses to date. We focus on a reach-scale study site, covering three meander bends and the adjacent floodplain. Morphological and terrestrial ecological data are combined under varying discharge conditions. The field study is performed in the context of stream restoration. Stream restoration projects are rarely subject to monitoring schemes combining morphological, hydrological and ecological surveys, although there are exceptions (e.g. Gurnell et al., 2006). The objective is to establish and understand the morphological response of a reconstructed lowland stream to riparian vegetation development and varying discharge conditions.

2 Study area

In October 2011 a stream restoration project was realized in the Lunterse Beek, representing a small lowland stream located in the central part of the Netherlands (52°4′46″ N, 5°32′30″ E) (see Fig. 1). A straightened channel was replaced by a new channel with a sinuous planform. The course of the new channel crosses the former channel at several locations (Fig. 1c). The new channel was constructed with a width of 6.5 m, a depth of 0.4 m and a longitudinal slope of 0.96 m km^{-1}. A lowered floodplain surrounded the channel, with an average width of 20 m. The bed material mainly consists of fine sand, with a median grain size of 258 µm (Eekhout, 2014).

Figure 1b shows the location of the study area in the catchment. The catchment covers an area of 63.6 km^2. The elevation within the catchment varies between 3 and 25 m above mean sea level. The study area is located in a lowland catchment, which implies a mild bed slope. The subsurface of the catchment mainly consists of aeolian-sand deposits. The average yearly precipitation amounts to 793 mm (KNMI, 2014). The average daily discharge amounts to

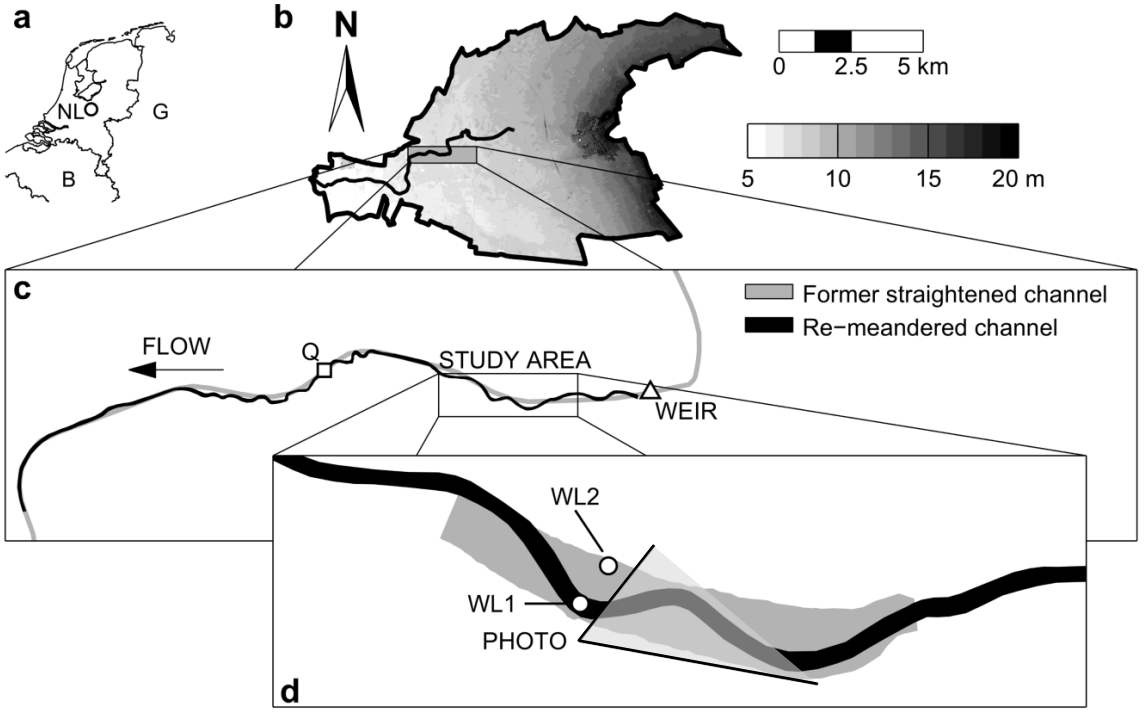

Figure 1. Overview of the study area: **(a)** location of the study area in the Netherlands; **(b)** elevation model of the catchment (Actueel Hoogtebestand Nederland, AHN; Van Heerd et al., 2000); **(c)** planform of the reconstructed reach, with the squared marker indicating the location of the discharge station (Q); and **(d)** sketch of the study area indicating the location of the water level gauges (WL1 and WL2) and the approximate extent of available terrestrial photographs (grey-shaded triangle, Fig. 9).

$0.33\,m^3\,s^{-1}$ and the peak discharge during the study period was $6.46\,m^3\,s^{-1}$.

A chute cutoff occurred within 3 months after realization of the stream restoration project, which is described in Eekhout (2014). Prior to the cutoff, a plug bar was deposited in the bend to be cut off. Hydrodynamic model results show that the location of the plug bar coincides with the region where flow velocity drops below the threshold of sediment motion, indicating the sediment deposition was caused by a backwater effect. Upstream from the plug bar, an embayment formed in the floodplain at a location where the former channel was located. The former channel was filled with sediment prior to channel reconstruction. The sediment fills originated from other parts of the study area, where excess sediment was available from the construction of the new channel. It is likely that the sediment at this location was less consolidated and therefore prone to erosion. The chute channel continued to incise and widen into the floodplain and, after 6 months, acted as the main channel, conveying the discharge during the majority of time.

3 Material and methods

3.1 Morphological Monitoring

The temporal evolution of the bathymetry has been monitored over a period of almost 2 years. Morphological data were collected in the area within the lowered floodplain over a length of 180 m, indicated in grey in Fig. 1d. Morphological data were collected with an average frequency of 52 days, using real-time kinematic (RTK) GPS equipment (Leica GPS 1200+ for surveys 1–13 and Leica Viva GS10 for survey 14). The RTK-GPS equipment allows for the surface elevation to be measured with an accuracy between 1 and 2 cm. The surface elevation data were collected along cross sections between the two floodplain edges. The survey strategy proposed by Milan et al. (2011) was followed, focusing on breaks of slope. Following this strategy, the point density was increased in the vicinity of steep slopes (e.g. channel banks), and decreased on flat surfaces (e.g. floodplains).

During five morphological surveys (1, 2, 4, 8 and an additional survey at day 687), bed elevation data were also obtained from 180 m upstream from the study area, over a length of approximately 350 m. These measurements were focused on the channel bed and provide information on the temporal evolution of the channel bed. The location of the crests of the channel bank in each cross section were marked

during the surveys. The channel bed elevation was obtained by subtracting the hydraulic radius from the average elevation of the two opposing crests of the channel banks. The hydraulic radius is defined as the cross-sectional area divided by the wetted perimeter.

3.2 DEM construction and processing

DEMs of each of the 14 datasets were constructed. The data were transformed to (s, n) coordinates using the method described by Legleiter and Kyriakidis (2007). Since the data were collected in cross sections, an anisotropy factor was used within the interpolation routine, accounting for dispersion of the collected data in the longitudinal direction. The anisotropy factor was determined by dividing the average streamwise distance between the subsequent cross sections by the average cross-stream distance between the individual point measurements. The data were split into a channel section and a floodplain section, to account for a higher density of point measurements in the channel than in the floodplain. A separate anisotropy factor was applied for the channel and the floodplain data. Table 1 lists the point density and anisotropy factors for all individual surveys, specified for the channel and floodplain sections.

The data were projected onto a curvilinear grid, following the channel centerline for the channel data and the valley centerline for the floodplain data. A triangular irregular network (TIN) was constructed using a Delaunay triangulation routine in Matlab, following Heritage et al. (2009). Subsequently, the TIN was interpolated onto a grid using nearest neighbour interpolation, with a grid spacing of 0.25 m. After interpolation, the data were transformed back to (x, y) coordinates. The interpolated channel and floodplain were then merged to facilitate the comparison between all 14 surveys.

Deposition and erosion patterns were obtained by subtracting two subsequent morphological surveys, yielding a DoD. Real morphological change can be different from apparent morphological change, which may arise from uncertainties in the individual DEMs, e.g. from instrumental errors or errors that arise from the interpolation routine. The uncertainty can be established by determining the threshold level of detection (LoD). The method by Milan et al. (2011) was adopted to construct the spatially distributed LoD. Milan et al. (2011) account for the increase of spatially distributed error in a DEM near steep surfaces (e.g. channel bank edges), by inferring the relationship between the standard deviation of elevation errors and local topographic roughness. The method by Milan et al. (2011) was adjusted, by adopting a single linear regression model to obtain the spatial standard deviation of elevation error grids. The regression model was obtained after combining elevation errors and local topographic roughness values, from all 14 surveys.

In each grid cell the LoD was obtained according to:

$$U_{\mathrm{crit}} = t\sqrt{(\sigma_{\mathrm{e},1})^2 + (\sigma_{\mathrm{e},2})^2} \quad (1)$$

Table 1. Overview of all morphological measurements, with point density (PD, points m^{-2}) and anisotropy factor (AF) as used in the interpolation routine, specified for the channel (ch.) and floodplain (fp.) areas, respectively.

Survey no.	Survey date (day)	No. data points	PD (all)	PD (ch.)	AF (ch.)	PD (fp.)	AF (fp.)
1	0	379	0.16	0.25	9.74	0.12	4.59
2	93	956	0.32	0.44	5.04	0.24	2.35
3	133	918	0.27	0.34	3.57	0.24	2.15
4	191	742	0.20	0.31	4.24	0.15	2.04
5	231	1158	0.30	0.45	4.19	0.24	2.09
6	288	1376	0.35	0.53	4.42	0.29	2.15
7	341	1296	0.32	0.50	4.04	0.26	1.86
8	377	1655	0.42	0.62	3.56	0.35	1.68
9	426	1484	0.39	0.58	3.50	0.31	1.64
10	454	1472	0.36	0.55	4.12	0.30	2.03
11	489	1420	0.35	0.51	4.08	0.29	2.05
12	525	1462	0.37	0.56	4.66	0.29	2.15
13	558	1256	0.31	0.50	4.08	0.24	1.77
14	672	1501	0.44	0.85	10.66	0.23	2.67

where U_{crit} is the critical threshold error, t is the critical Student's value and $\sigma_{\mathrm{e},1}$ and $\sigma_{\mathrm{e},2}$ are the standard deviation of elevation error, for the first and second survey, respectively. The threshold value is based on a critical Student's t value, at a chosen confidence level. Following Milan et al. (2011), a confidence limit equal to 95 % was applied, which results in $t \geq 1.96$ (2σ). The elevation difference between two subsequent surveys at a particular grid cell is insignificant when $z_{i,j}(\mathrm{new}) - z_{i,j}(\mathrm{old}) < U_{\mathrm{crit}}$, where $z_{i,j}(\mathrm{new})$ and $z_{i,j}(\mathrm{old})$ are the elevations of the two subsequent morphological surveys at grid cell (i, j). A lower bound for the critical threshold error was adopted, to account for the accuracy of the RTK-GPS equipment. This lower bound was set to $U_{\mathrm{crit}} = 0.04$ m, which is 2 times the maximum error of the RTK-GPS equipment.

3.3 Quantifying morphological activity

For each DoD, the morphological activity was quantified for the study area as a whole and for isolated geomorphic zones. In each individual DEM, the study area was segregated into four geomorphic zones: channel bank, channel bed, floodplain and cutoff channel. Figure 2a shows an example of the distribution of each of the four geomorphic zones in the study area for the period between surveys 4 and 5, days 191–231. Segregation of each of the four geomorphic zones was accomplished as follows. The channel bank mask is defined as the zone between the channel bank lines of two subsequent surveys plus a strip of 0.5 m width on either side of the zone. The channel bed mask is defined as the zone between the two channel bank masks. The remainder of the grid domain is labelled as floodplain, with the cutoff channel considered as

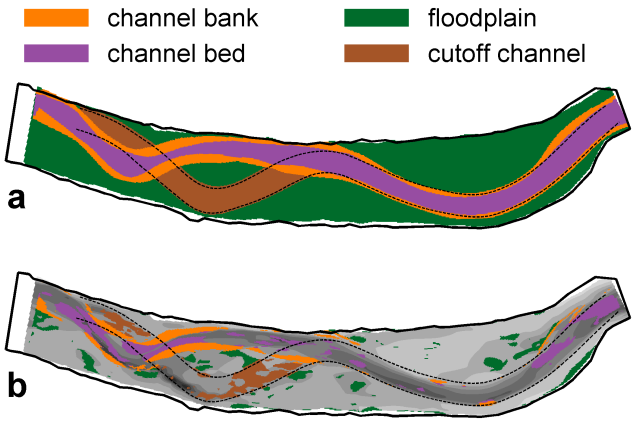

Figure 2. Segregation of geomorphic zones between surveys 4 and 5. **(a)** Masks of each of the four geomorphic zones, including channel bank (orange), channel bed (purple), floodplain (green) and cutoff channel (brown). **(b)** Resulting segregation.

a separate geomorphic zone. Finally, each of the patches of morphological change was attributed to one of the geomorphic features (Fig. 2b).

Two methods were applied to quantify morphological activity. First, the volumetric change in sediment storage was determined. Volumetric change in sediment storage was determined by integrating elevation change over area, distinguishing between gross erosion and gross deposition. Net sediment change was determined by subtracting gross erosion from gross deposition. The uncertainty associated with the volumetric change in sediment storage were estimated using the method described by Wheaton et al. (2013), who defined the uncertainty as plus or minus one standard deviation of the volumetric error. The latter standard deviation is approximated from the error surface, obtained from the LoD method (Milan et al., 2011), as the sum of squared errors.

Second, the root-mean-square elevation (RMSD, m) difference was determined:

$$\mathrm{RMSD} = \sqrt{\frac{\sum \left[z_{i,j}(\mathrm{new}) - z_{i,j}(\mathrm{old})\right]^2}{n}}, \quad (2)$$

where $z_{i,j}$ is the elevation in grid cell (i, j) of the DEM and n is the number of grid cells. The volumetric change in sediment storage and the RMSD were expressed as a rate of change by dividing both quantities by the time between two successive surveys.

3.4 Hydrological monitoring

Discharge data were collected downstream of the study reach at a discharge measurement weir, indicated by Q in Fig. 1c. Discharge estimates were acquired with a 1 h frequency. Water level data were collected at a water level gauge in the study area, indicated by WL1 in Fig. 1d. Initially, the water level gauge was placed in the channel that became subject to cutoff. After day 288, the water level gauge was moved to a new location, on the other side of the floodplain, indicated by WL2 in Fig. 1d. Water level data were acquired with a 1 h frequency. Due to a malfunctioning pressure sensor, water level data were unavailable in the first 103 days after channel reconstruction. Longitudinal water level profiles were measured with RTK-GPS equipment during 13 of the 14 morphological surveys.

3.5 Linear regression modelling

To investigate the degree to which morphological activity responds to discharge variation, values of the RMSD were related to time-averaged dimensionless bed shear stress (Shields stress). The Shields stress θ (–) is defined as

$$\theta(t) = \frac{S_\mathrm{w} R(t)}{d_{50} s}, \quad (3)$$

where S_w is the longitudinal water level slope (–); $R(t)$ is the hydraulic radius (m); and $s = (\rho_s - \rho)/\rho$ is the relative submerged specific gravity of the sediment (–), with $\rho = 1000\,\mathrm{kg\,m^{-3}}$ the density of water and $\rho_s = 2650\,\mathrm{kg\,m^{-3}}$ the density of sediment. The average longitudinal water level slope S_w was used, amounting to $0.49\,\mathrm{m\,km^{-1}}$. The average value was calculated from the last 11 water level profiles from the morphological surveys, excluding the two pre-cutoff water level profiles. The hydraulic radius $R(t)$ was obtained by dividing the cross-sectional flow area $A(t)$ by the wetted perimeter $P(t)$, obtained from the cross section at the location of the water level gauge. Equation 3 was applied to the discharge and water level time series and averaged between two successive morphological surveys in order to obtain an estimate of the time-averaged Shields stress per period.

3.6 Riparian vegetation

The restored stream was constructed in bare soil. Riparian vegetation started to develop halfway through the first year. The temporal development of the riparian vegetation was monitored by means of field surveys, aerial photographs and oblique terrestrial photographs.

Coverage of riparian vegetation species were estimated during two field surveys, at day 339 (September 2012) and day 645 (July 2013). The surveys were performed in three cross sections: at 17, 84, and 120 m upstream from the study area. In each cross section, species cover was mapped visually by estimating the vertical projection of a species' shoot area to the soil surface. Species cover was mapped in five rectangular plots (25 cm × 50 cm), located on the channel bed (1 plot), at the channel bank toe (1 plot), in the floodplain (2 plots) and on the floodplain edge (1 plots). Data from two plots per cross section were used to estimate the dominant riparian vegetation species. The two plots were located in

the floodplain, at 2.7–5.5 and 7.9–11.7 m from the channel banks.

The spatial distribution of the riparian vegetation was obtained from three aerial photographs, taken at day 188 (April 2012), day 289 (July 2012) and at day 636 (July 2013). The aerial photographs were taken with a 10 cm (day 188) and 25 cm (days 289 and 636) resolution. Figure 3a shows an example of the aerial photograph taken at day 289. The last two aerial surveys included colourized infrared (CIR) images (Fig. 3b), which contain data from the near-infrared (NIR) wavelengths (0.78–3 µm). With these data the riparian vegetation development at these two dates was quantified with the normalized difference vegetation index (NDVI):

$$\mathrm{NDVI} = \frac{\mathrm{NIR} - \mathrm{VIS}}{\mathrm{NIR} + \mathrm{VIS}}, \quad (4)$$

where NIR is the intensity of the NIR wavelengths and VIS is the intensity of the visible red wavelengths. Equation 4 was applied to the entire image, from which the spatial variation of the NDVI within the study area was obtained. NDVI varies between −1.0 and 1.0. Positive values generally correspond to vegetation, whereas negative values correspond to water or other media that adsorb the infrared wavelengths (Clevers, 1988).

Figure 3c shows the NDVI from the second aerial survey for the study area and surrounding agricultural fields and roads. The panel clearly shows positive values for the pasture area on the north side of the study area. Negative values are obtained inside the channel and on the road, on the south side of the study area. The obtained NDVI values within the study area are in a range between 0 and 0.2, which is associated with bare soil (Holben, 1986). Nevertheless, the aerial photo and field observations show that riparian vegetation was present in the study area, where higher NDVI values corresponded to more abundant riparian vegetation. Further analysis of the aerial photographs only considers the areas where positive NDVI values are obtained.

Oblique terrestrial photographs were taken during the majority of the morphological surveys. The series of photographs provide a qualitative view on the temporal development of the riparian vegetation in the study area.

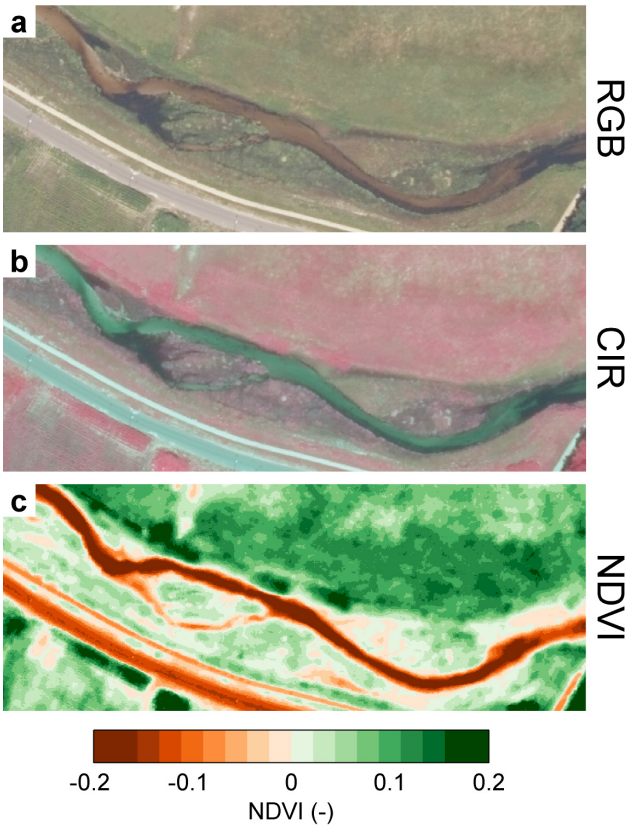

Figure 3. An example of the second aerial photograph (day 289) from which the NDVI was determined, showing **(a)** the RGB image (red, green, blue), **(b)** the CIR image (colourized infrared) and **(c)** the NDVI. In **(c)**, the green-coloured areas indicate positive NDVI values, and orange-coloured areas indicate negative NDVI values. All images have a 25 cm resolution.

4 Results

4.1 Morphodynamics

Figures 4 and 5 show, respectively, the DEMs and DoDs of the 14 morphological surveys. The first three surveys (days 0, 93 and 133) show the sequence of morphological changes that capture the chute cutoff event. The first DoD (day 0–93) shows deposition of sediment on the channel bed, which is associated with the formation of a plug bar (Eekhout, 2014). An initial embayment had formed upstream from the bend to be cutoff. The actual cutoff occurred in the second period (day 93–133), where a new channel incised into the floodplain. In the subsequent period (day 133–231), the morphological changes occurred mainly in the bend at the downstream end of the study area. During this period, both erosion of the outer bank and accretion in the inner bank were observed in this bend. Subsequently, there was a period of little morphological change (day 231–288). In the last period (day 341–672), morphological changes were restricted to the channel bed and banks. At that time, little morphological change was observed in the floodplain.

Overall, most morphological developments were observed in the downstream half of the study area. Figure 4 clearly illustrates the channel bed incision of the bend at the downstream end of the study reach in the period following the chute cutoff. The upstream half of the study reach did not show pronounced morphological changes. Apart from occasional changes in the channel bed, no structural bank erosion or accretion was observed.

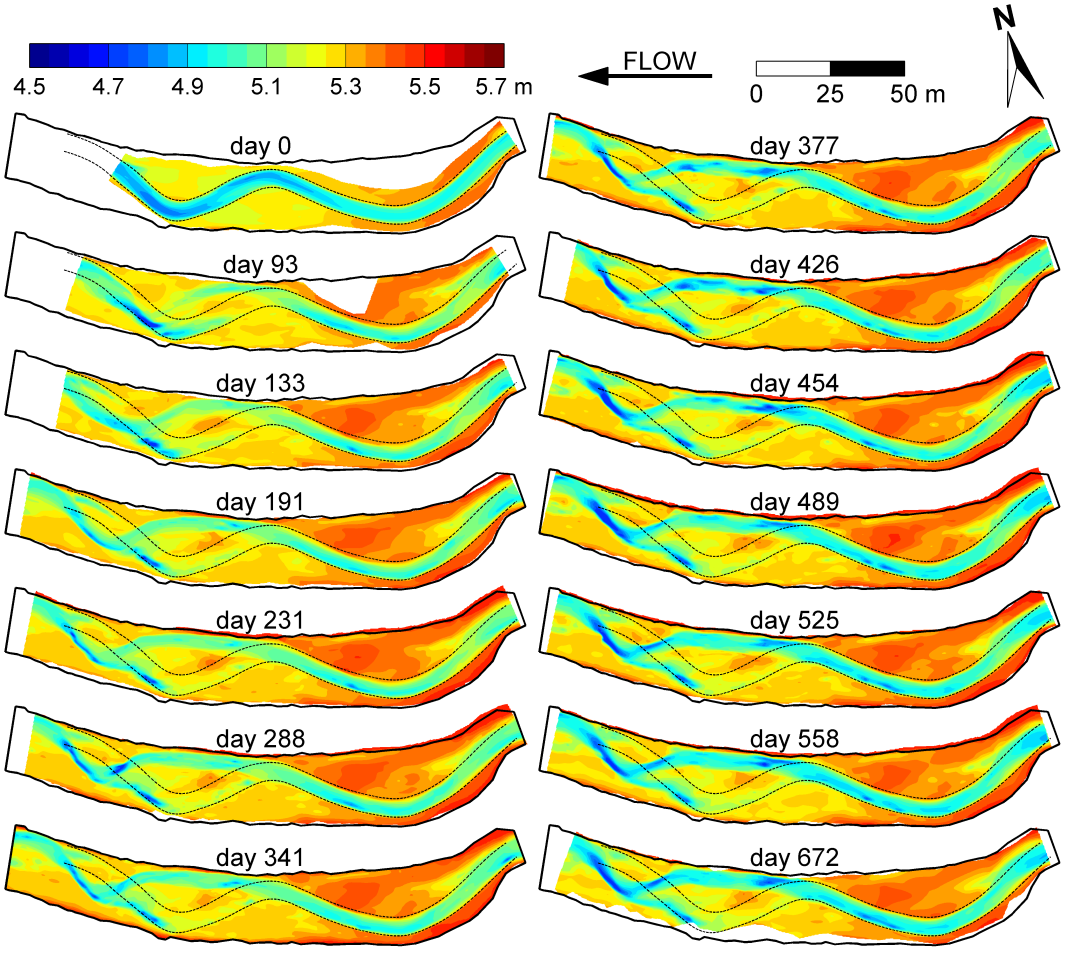

Figure 4. DEMs of all 14 morphological surveys. The number of days indicate the time since channel reconstruction. The dashed black lines indicate the location of the channel banks of the reconstructed channel. The solid black line surrounding the DEMs indicates the extent of the seventh morphological survey (day 341). Elevation is indicated in metres above mean sea level.

Figure 6 and Table 2 show the sediment budgets, derived from the DoDs (Fig. 5). Figure 6a shows volumetric change over the study area as a whole, aggregated for regions of erosion and deposition as well as net change. Figure 6b shows the volumetric change subdivided per geomorphic zone. Considering the study area as a whole (Fig. 6a), a shift from net deposition to net erosion is observed. In the first period (between surveys 1 and 2), deposition is mainly caused by the deposition of sediment in the channel bed and in the cutoff channel. This is followed by a period of limited net change between surveys 2 and 4, where bank erosion is balanced by net deposition in the rest of the study area. From the fifth survey onwards, the sediment balance shifts towards net erosion. Channel bed processes (channel bed incision) are the dominant contributors to the net erosion of sediment in the study area.

Figure 6a shows that net deposition occurred in the periods between surveys 1 and 2 as well as surveys 4 and 5. This implies that sediment was transported towards the study area from upstream. This observation is confirmed by Fig. 7, which shows longitudinal channel bed elevation data obtained over an area ranging from a distance of 180 m upstream from the study area to the downstream end of the study reach. The figure shows that between days 0 and 93, upstream channel bed incision led to channel bed aggradation in the downstream part. In the upstream area only minor changes in channel bed elevation occurred in the period following day 93. The deposited sediment in the study area gradually eroded, which explains the negative sediment balance in several periods between surveys 5 and 14 (Fig. 6a).

4.2 Riparian vegetation development

Table 3 lists the dominant (average cover $> 10\,\%$) riparian vegetation species and their characteristics obtained from two field surveys. The dominant species in 2012 were *Juncus articulatus* (jointed rush) and *Juncus bufonius* (toad rush). *Juncus articulatus* was also among the dominant species in 2013, together with *Juncus effusus* (soft rush) and *Trifolium*

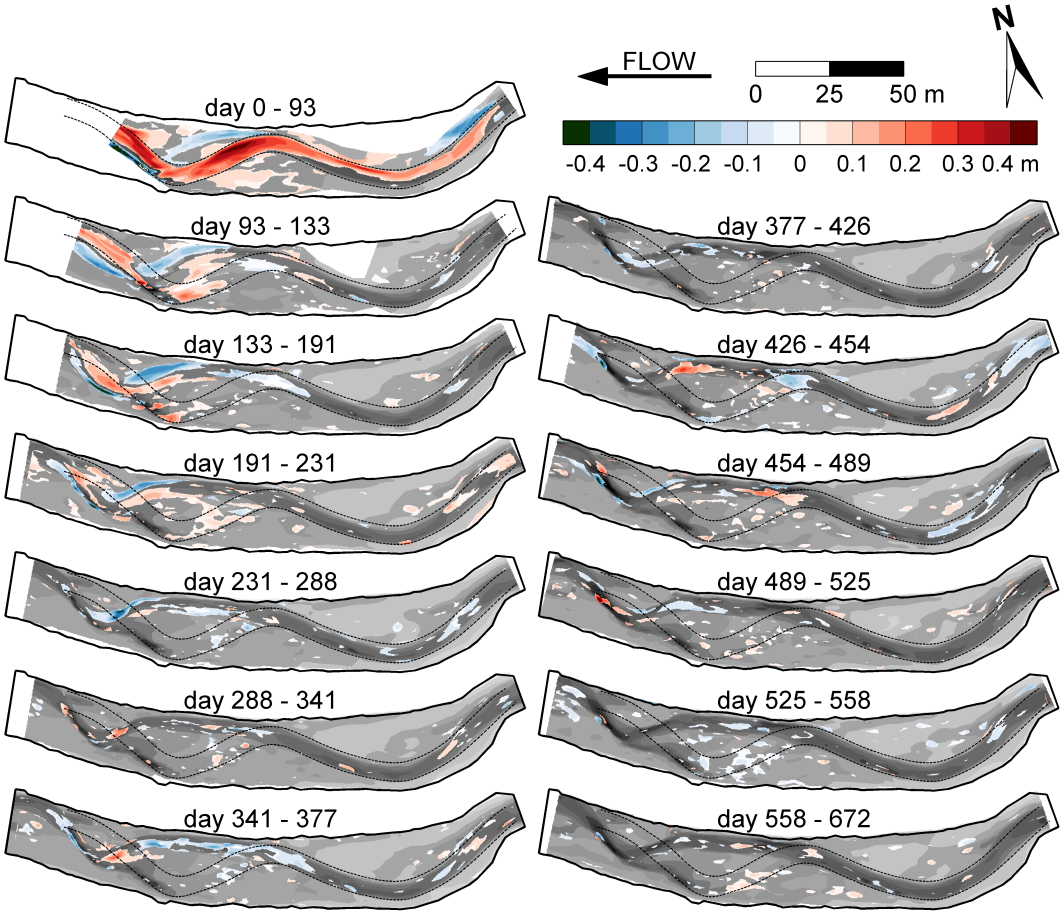

Figure 5. DoDs of all 13 periods between the 14 morphological surveys. The number of days indicates the time since channel reconstruction. The dashed black lines indicate the location of the channel banks of the reconstructed channel. The solid black line surrounding the DEMs indicates the extent of the seventh morphological survey (day 341). Erosion is indicated in blue and deposition in red. The DEM of the first of the two DEMs is shown in greyscale.

repens (white clover). All species are classified as herbaceous vegetation and are perennial. The growing season of the dominant species is roughly from June to September, which explains the maximum coverage in September as observed in Fig. 9 (days 341 and 672). Maximum root depth varies between less than 10 cm and 100 cm. The presented root depth values are valid for fully grown specimens. It is likely that the root depths for the observed riparian vegetation in this case study were shorter.

Figure 8 shows the three aerial photographs and the derived positive NDVI values for the last two aerial surveys. Panel a shows that riparian vegetation was absent in the study area at day 188. The second aerial photograph (day 289, panels b and d) shows that a patchy pattern of riparian vegetation started to emerge in the floodplain area. At the time of taking the second aerial photograph, riparian vegetation cover (observed as a positive NDVI value) amounted to 56 % of the study area. Specified per geomorphic zone, riparian vegetation covered 33 % of the channel bank zone, 3 % of the channel bed zone, 80 % of the floodplain zone and 57 % of the cutoff channel zone. Riparian vegetation in the cutoff channel did not develop as abundantly as in the rest of the floodplain. There is also a clear distinction between channel (bed and bank) and floodplain. The third aerial photograph (day 636, panels c and e) clearly shows that riparian vegetation cover increased from the first to the second year, when riparian vegetation cover amounted to 77 % of the study area. Riparian vegetation cover increased in all geomorphic zones, amounting to 84 % of the channel bank zone, 22 % of the channel bed zone, 97 % of the floodplain zone and 92 % of the cutoff channel zone.

Figure 9 shows the series of 14 oblique terrestrial photographs taken from the location indicated in the lower-right corner of the figure. Just after channel reconstruction had finished at day 0 (first photo on row one), riparian vegetation was visible on the left channel bank. Overall, riparian vegetation was absent in the floodplain. In the subsequent period, until day 161 (third photo on row one), no change in

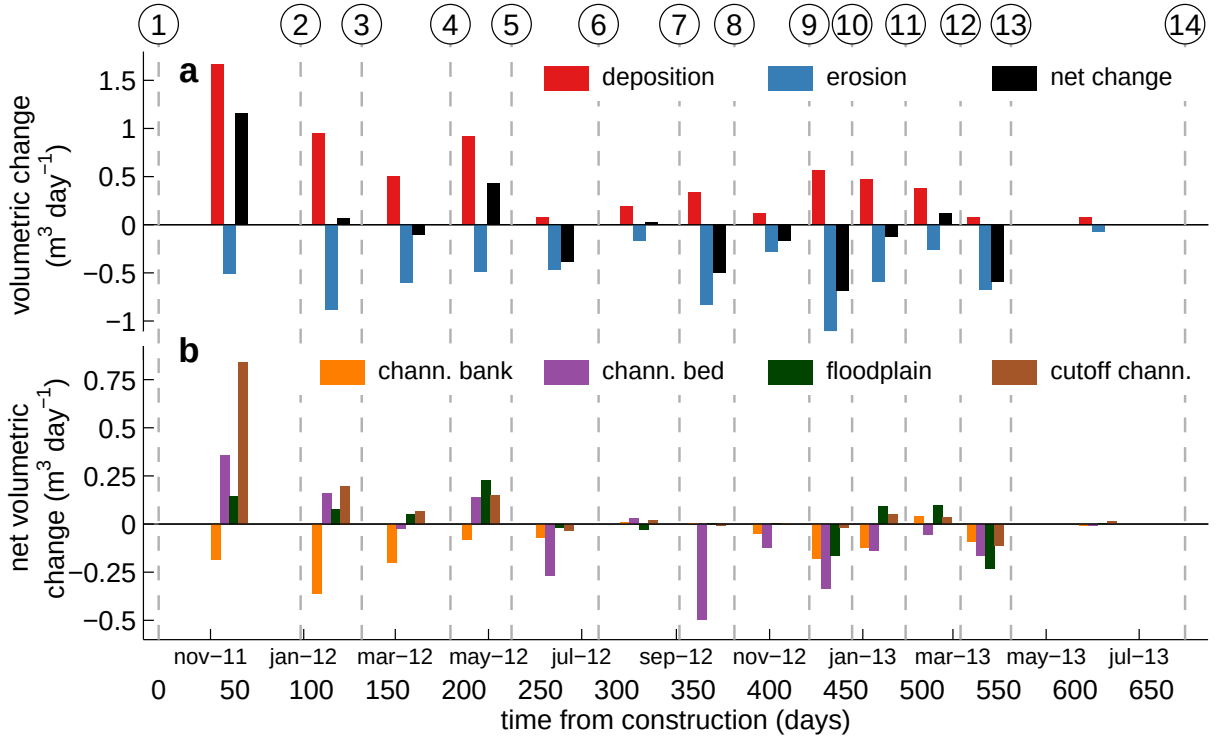

Figure 6. Temporal evolution of the volumetric change in sediment storage. **(a)** Volumetric change in sediment storage ($m^3\,day^{-1}$) for regions of deposition (red), erosion (blue) and net change (black). **(b)** Volumetric change in sediment storage ($m^3\,day^{-1}$), specified per geomorphic feature, with channel bank (orange), channel bed (purple), floodplain (green) and cutoff channel (brown). The dashed vertical lines indicate the surveying moments, and the numbers at the top of the figure correspond to the numbers in Table 1.

Table 2. Summary of volumetric change in storage by deposition, erosion and net change (deposition minus erosion). Volumetric change is specified in gross change ($\sum$ volume) and the standard deviation (SD).

Period (days)	Deposition $\sum$ volume $\pm$ SD (m^3)	Erosion $\sum$ volume $\pm$ SD (m^3)	Net change $\sum$ volume $\pm$ SD (m^3)
0–93	155.1 ± 23.5	-47.2 ± 7.9	107.9 ± 31.4
93–133	38.1 ± 8.0	-35.2 ± 6.4	2.9 ± 14.4
133–191	29.1 ± 7.1	-35.2 ± 6.7	-6.0 ± 13.8
191–231	36.8 ± 10.9	-19.7 ± 4.3	17.2 ± 15.2
231–288	4.4 ± 1.5	-26.4 ± 7.3	-22.0 ± 8.8
288–341	10.1 ± 3.2	-8.9 ± 2.9	1.2 ± 6.1
341–377	12.2 ± 3.4	-30.0 ± 8.8	-17.9 ± 12.2
377–426	5.8 ± 2.1	-13.7 ± 4.6	-7.9 ± 6.7
426–454	15.9 ± 4.6	-35.2 ± 9.5	-19.3 ± 14.1
454–489	16.4 ± 5.1	-20.7 ± 6.7	-4.3 ± 11.8
489–525	13.6 ± 4.7	-9.4 ± 3.3	4.2 ± 8.0
525–558	2.7 ± 1.0	-22.2 ± 7.7	-19.5 ± 8.7
558–672	9.0 ± 2.9	-8.6 ± 3.2	0.3 ± 6.2

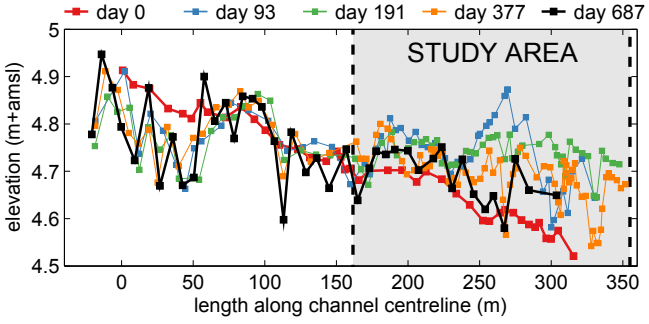

Figure 7. Temporal evolution of the longitudinal bed elevation.

riparian vegetation coverage was observed. Riparian vegetation started to develop around day 231 (last photo on row one). Some patches of riparian vegetation were emerging in the floodplain and on the channel banks. The development of riparian vegetation continued in the following period and a maximum riparian vegetation coverage was observed at day 341 (second photo on row two). At that time, the floodplain was almost entirely covered with riparian vegetation. Only in the cutoff channel did riparian vegetation develop less abundantly (see also Fig. 8d). In the period until the end of the study period, from day 377 (third photo on row two) until day

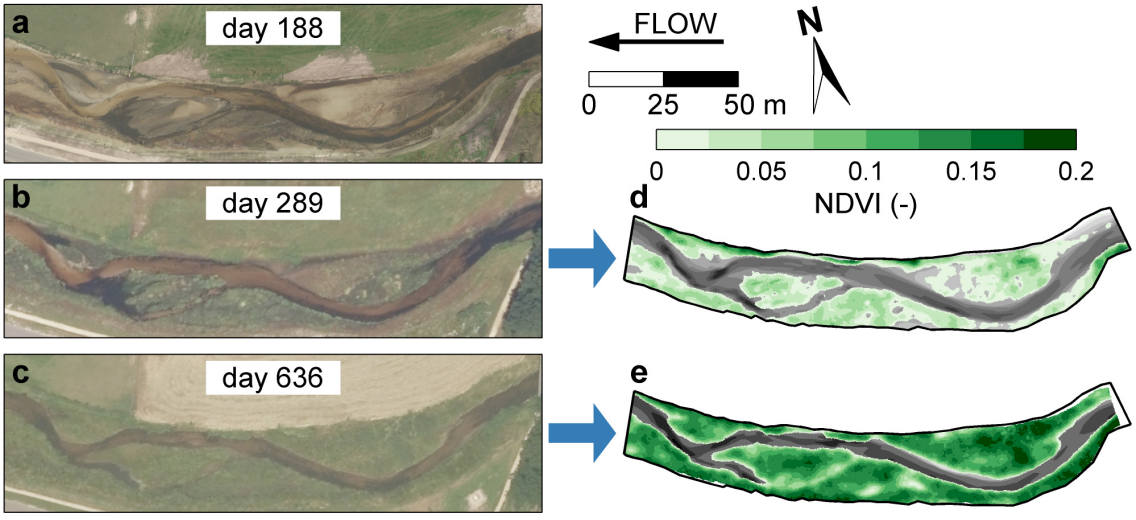

Figure 8. Three aerial photographs taken on **(a)** day 188 (April 2012), **(b)** day 289 (July 2012) and **(c)** day 636 (July 2013); **(d)** and **(e)** show positive NDVI values derived from the aerial photographs from **(b)** and **(c)**, respectively. The DEMs from survey 6 **(d)** and survey 13 **(e)** are shown in greyscale as a reference.

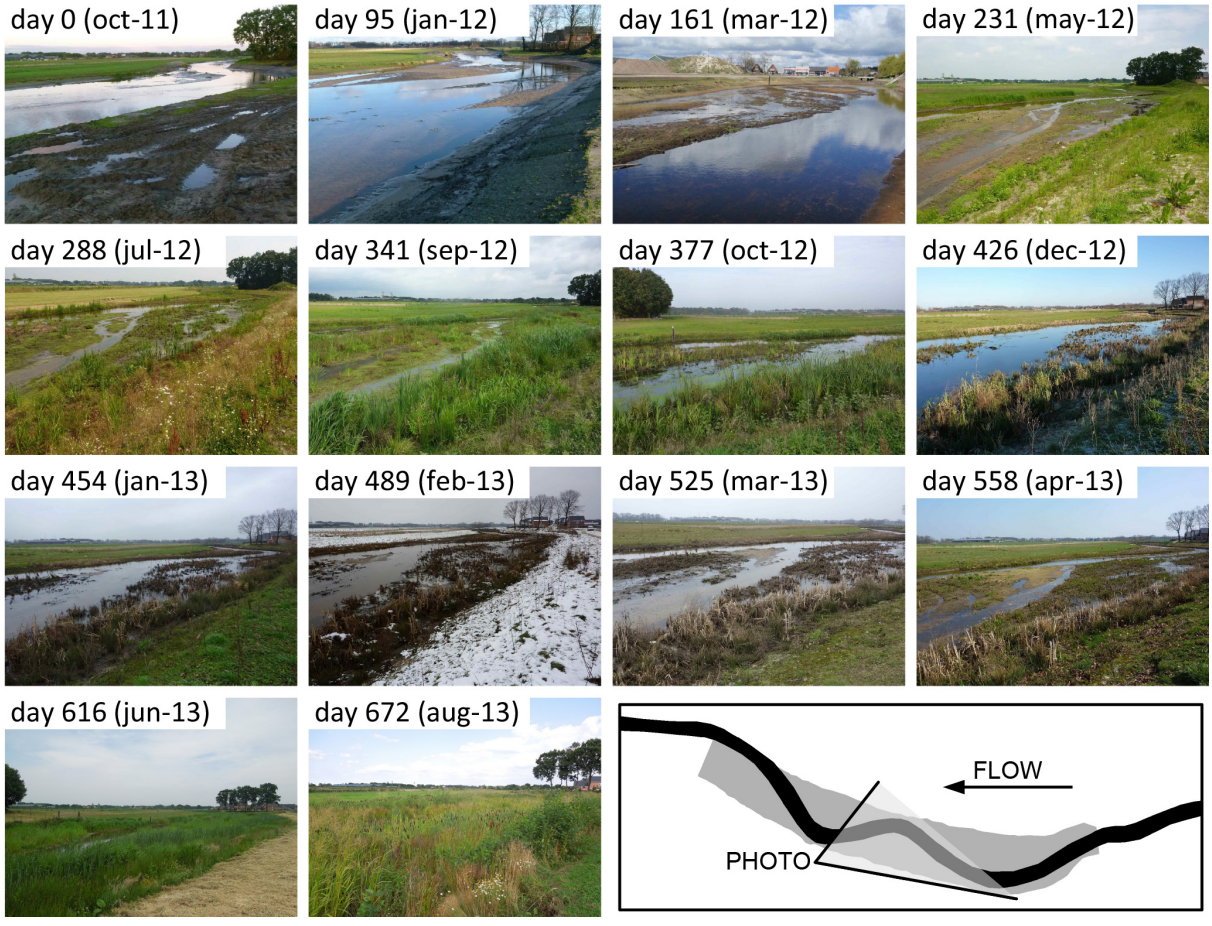

Figure 9. Series of 14 oblique terrestrial photographs taken from the location indicated in Fig. 1d, except for the third photo (day 161), which was taken from the other side of the floodplain.

Table 3. Characteristics of the most dominant riparian vegetation species found in the floodplain, including average cover (%), lifetime, growing season and maximum root depth. The presented characteristics were obtained from http://www.wilde-planten.nl/ (*Wilde planten in Nederland en België* – Wild plants in the Netherlands and Belgium).

Scientific name	Cover (%)	Lifetime	Growing season	Root depth
September 2012				
Juncus articulatus	19	Perennial	Jun–Sep	10–20 cm
Juncus bufonius	22	Annual	Jun–Sep	< 10 cm
July 2013				
Juncus articulatus	14	Perennial	Jun–Sep	10–20 cm
Juncus effusus	14	Perennial	Jun–Aug	< 100 cm
Trifolium repens	28	Perennial	May–Oct	10–50 cm

558 (last photo on row three), the riparian vegetation cover started to decrease to a level approximately similar to the situation between days 231 and 288. The riparian vegetation cover started to increase again from day 558 onwards. This resulted in the maximum riparian vegetation cover at the end of the survey period, at day 672 (second photo on row four).

4.3 Morphodynamic regime change

Figure 10 combines the data obtained from the morphological surveys, oblique terrestrial photographs and discharge measurements. Figure 10a shows morphological change (RMSD, m year^{-1}), which has been derived from Fig. 5, with Eq. 2. Figure 10b shows the discharge hydrograph, obtained from the measurement weir located 360 m downstream from the study area (Fig. 1c). The temporal evolution of the morphological change (black diamonds in Fig. 10a) shows that the RMSD metric of morphological change was relatively high in the first two periods, between surveys 1 and 3. In the subsequent period, morphological changes show a decreasing trend until the period between surveys 6 and 7. In the final period, incidental peaks are observed during periods of increased discharges, i.e. in periods between surveys 7 and 8 as well as surveys 9 and 10.

From Fig. 10a it appears that the study period can be divided into two stages. The first stage can be considered an apparent morphological disequilibrium. The interval between surveys 1 and 3 is largely dominated by the chute cutoff event, which is followed by an interval until survey 5 that is dominated by channel bank processes. During the second stage, the morphology within the study reach can be considered to tend towards an equilibrium, in the sense that the reach-scale morphology has largely stabilized. Both channel bank and channel bed processes dominate morphological change in the latter stage. During the whole study period, morphological changes in the floodplain contributed only slightly to the overall changes in the study area.

The temporal development of riparian vegetation, indicated by the green shading in Fig. 10, shows reach-scale riparian vegetation development from day 231 onwards. An initial maximum riparian vegetation coverage is observed in the period between surveys 7 and 8, which corresponds to the photo taken on day 341 (Fig. 9, second photo on row two). In the subsequent period, until survey 13, a decrease of riparian vegetation cover is observed. A second maximum riparian vegetation coverage is observed in the period following survey 14, which corresponds to the photo taken on day 672 (Fig. 9, second photo on row four). Figure 10b shows that two periods of extremely high discharges occurred, i.e. in the periods between surveys 1 and 2 and surveys 9 and 10, featuring discharge peaks with a return period of 120 days and 180 days per year^{-1}, respectively.

Figure 10 shows an initial stage of morphological disequilibrium, when rates of morphological change are relatively high without showing a clear response to discharge variation. In the subsequent near-equilibrium stage, a clear response to the varying discharge is evident. A linear regression model was established, relating the RMSD to time-averaged Shields stress for the study area as a whole. The linear regression model was established for the period after riparian vegetation emerged (between surveys 5 and 14) only. The evaluation was based on the hypothesis that morphological activity in the period prior to riparian vegetation growth was significantly different from the period after riparian vegetation emerged. Additionally, the 95 % confidence interval was determined based on the Student t distribution, with the degrees of freedom corresponding to the number of periods after riparian vegetation emerged.

Figure 11 shows the results from the linear regression between RMSD and time-averaged Shields stress. The RMSD in a certain period is significantly different from predicted values when the value is outside the 95 % confidence interval. Considering the study area as a whole, the period prior to riparian vegetation growth is outside the 95 % confidence interval. These results indicate that the morphodynamic behaviour during the period prior to riparian vegetation growth is significantly different from the period after riparian vegetation emerged.

5 Discussion

Figures 4 and 5 show that active meander processes occurred in the initial period prior to riparian vegetation growth, including a chute cutoff and meander migration. In the subsequent period, when riparian vegetation started to emerge, the active meander processes were less pronounced, although localized bank erosion was observed. From Fig. 6 and Table 2 it appears that the study period can be subdivided into an initial period of net deposition (prior to survey 5) and a subsequent period of net erosion (after survey 5).

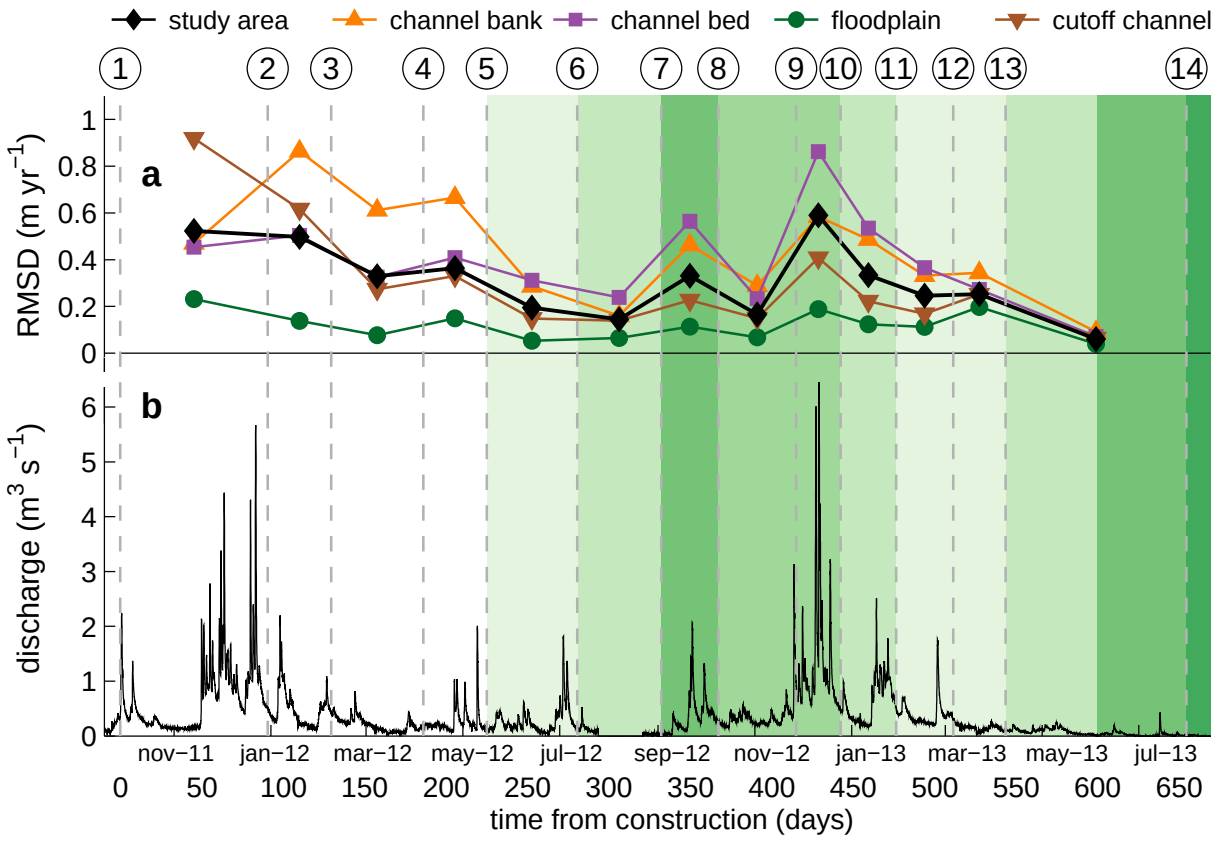

Figure 10. Temporal evolution of **(a)** the rate of morphological change (m year^{-1}) for the study area as a whole (black diamonds) and specified per morphological feature, with channel bank (orange triangles), channel bed (purple squares), floodplain (green circles) and cutoff channel (brown triangles), as well as **(b)** discharge hydrograph (m^3 s^{-1}). The green shading indicates the riparian vegetation coverage, estimated from Fig. 9. The dashed vertical lines indicate the surveying moments, and the numbers at the top of the figure correspond to the numbers in Table 1.

Figure 7 shows that in the period between surveys 1 and 2 upstream channel bed incision caused channel bed aggradation in the study area. The active meandering processes, as observed in the period prior to riparian vegetation growth, may be related to the associated net sediment accumulation. Variation in sediment supply has been previously related to differences in morphological regime. An increased sediment supply in a river may result in braided or actively meandering planforms, including chute cutoffs, whereas reduced sediment supply may result in laterally stable, sinuous planforms (Church, 2006; Kleinhans, 2010). In the present case study, the regime difference between the two periods may partially be explained by the difference in sediment supply. In the initial period, the channel may have acted as an actively meandering river, as a consequence of excessive sediment supply. After the sediment supply reduced, the channel may have acted as a laterally stable, sinuous river. The marked difference between the two periods of morphological behaviour may also relate to the growing season of the observed riparian vegetation. It is infeasible to isolate the role of reduced upstream sediment supply from the effect of riparian vegetation development; both factors may assert a substantial influence on the morphological regime change.

The dominant riparian vegetation species are all classified as herbaceous vegetation. The root structure of herbaceous vegetation differs from other vegetation types, such as shrubby and woody vegetation. Herbaceous vegetation shows a more graminoid-shaped root structure, including fibrous roots (Wynn et al., 2004; Burylo et al., 2011), as opposed to shrubby and woody vegetation, which include a taplike root system without fibrous roots (Burylo et al., 2011). These differences in root structure cause differences in erosional resistance. Recent studies have shown that herbaceous vegetation provides more soil reinforcement and is more efficient in improving aggregate stability than shrubby and woody vegetation (Burylo et al., 2011; Fattet et al., 2011). The advantages of erosion resistance for herbaceous vegetation are most effective in the top soil layer (< 30 cm; Wynn et al., 2004). Herbaceous vegetation types are among the first to (re-)colonize the substrate after environmental disturbance or land restoration (Cammeraat et al., 2005; Burylo et al., 2007). Although most of the studies supporting this

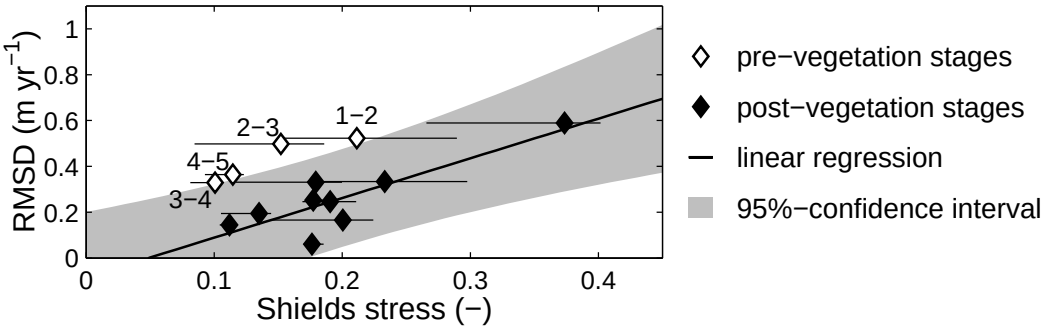

Figure 11. Linear regression between time-averaged Shields stress (–) and the root-mean-square elevation difference (RMSD, m year^{-1}) for the study area as a whole. The open and filled markers correspond to the pre-vegetation and post-vegetation stages, respectively. The solid black line denotes the linear regression curve for the period after riparian vegetation emerged (between surveys 5 and 14). The grey-shaded area indicates the extent of the 95 % confidence interval of the regression model. The extent of the black horizontal lines indicate the 25 % and 75 % quantiles.

were performed in different geographical regions and within different climates, these results show that herbaceous vegetation may have a significant impact on soil stability in the study area. The influence of herbaceous vegetation on bank stability may be particularly relevant for lowland streams due to their low channel depths. The temporally high rate at which riparian vegetation has colonized the lowered floodplains confirms a previous study by Gurnell et al. (2006).

For future research, it may be worthwhile better quantifying the rate at which riparian vegetation colonizes the floodplain and channel banks after stream restoration measures are implemented. If riparian vegetation indeed effectively fixes the channel banks, which cannot be clearly demonstrated from this study, riparian vegetation may exert an influence on hydraulic geometry relations in the equilibrium state. Hydraulic geometry theory quantifies scale relations between channel depth, width, mean flow velocity and bed slope in alluvial rivers and streams, which is often used in stream restoration practice (Rosgen, 1994; Copeland et al., 2001; Shields et al., 2003). For rivers, such scaling relations generally do not account for riparian vegetation (Wilkerson and Parker, 2011). For streams with channel depths similar to root depths, such as lowland streams, hydraulic geometry relations may be much dependent on riparian vegetation species, and on the timing of the grow season relative to the discharge hydrograph. It is not unlikely that details in the first year after reconstruction of a stream are crucial for the terminal channel geometry.

6 Conclusions

A detailed monitoring plan was implemented to monitor a lowland stream for a period of almost 2 years after channel reconstruction. Morphological, hydrological and ecological data were combined to establish interactions between reach-scale morphodynamics, discharge dynamics and riparian vegetation development. In the initial stage after channel reconstruction, when negligible riparian vegetation was present, channel morphology adjusted rapidly towards an alternative, complex topography. This period can be characterized by the occurrence of a chute cutoff and large-scale bank erosion. Upstream sediment supply may have played a substantial role in the initial morphological development in the study area. Riparian vegetation emerged in the subsequent stage. Channel bed incision and localized bank erosion dominate the morphodynamic developments after riparian vegetation had developed. Linear regression analysis shows that the morphological response to Shields stress variation is significantly different between the pre-vegetation and post-vegetation stages, and hence a morphological regime change had occurred.

The two stages of morphological adjustments reveal the rate at which a lowland stream adjusts towards a new morphological equilibrium. The two stages of morphological response may be largely associated with upstream sediment supply, caused by channel incision upstream from the study area. From the obtained field evidence, the role of riparian vegetation in the morphological regime change cannot be isolated from the effect of reduced sediment supply. The characteristics of the herbaceous vegetation and channel dimensions of lowland streams suggest that the initial riparian vegetation may exert a significant control on the stability of the channel banks. It may be worthwhile minimizing the duration of the initial stage of morphological adaptations after a lowland stream restoration project is realized. To some extent, this duration can be manipulated by changing the season in which the new channel is planned to be reconstructed. This has an impact on the duration of the pre-vegetation period, when the channel-forming discharges may cause significant morphological changes. In streams where channel depths are similar to root depths, the developments of riparian vegetation growth in the first years may be decisive for the terminal morphological equilibrium.

Acknowledgements. This study is part of a research project funded by the STOWA, the Foundation for Applied Water Research (project code 443209), and the research project Beekdalbreed Hermeanderen funded by Agency NL (project code KRW 09023) and co-funded by STOWA. We thank Philip Wenting (Wageningen University) and Andrés Vargas-Luna (Deltares) for their contribution to the fieldwork campaign, and Paul Torfs (Wageningen University) for his help in post-processing of field data. We thank CycloMedia Technology B.V. and Slagboom en Peeters Luchtfotografie B.V. for providing the aerial photographs. Also, we thank Remko Uijlenhoet (Wageningen University), Piet Verdonschot (Alterra), Christian Huising (Waterschap Vallei en Veluwe), Simon Dixon (University of Birmingham) and two anonymous reviewers for their comments on the manuscript. The morphological and hydrological data are made available through doi:10.6084/m9.figshare.960038.

Edited by: F. Metivier

References

Abernethy, B. and Rutherfurd, I. D.: The distribution and strength of riparian tree roots in relation to riverbank reinforcement, Hydrol. Process., 15, 63–79, 2001.

Brasington, J., Langham, J., and Rumsby, B.: Methodological sensitivity of morphometric estimates of coarse fluvial sediment transport, Geomorphology, 53, 299–316, doi:10.1016/S0169-555X(02)00320-3, 2003.

Braudrick, C. A., Dietrich, W. E., Leverich, G. T., and Sklar, L. S.: Experimental evidence for the conditions necessary to sustain meandering in coarse-bedded rivers, P. Nat. Acad. Sci. USA, 106, 16936–16941, doi:10.1073/pnas.0909417106, 2009.

Burylo, M., Rey, F., and Delcros, P.: Abiotic and biotic factors influencing the early stages of vegetation colonization in restored marly gullies (Southern Alps, France), Ecol. Eng., 30, 231–239, doi:10.1016/j.ecoleng.2007.01.004, 2007.

Burylo, M., Hudek, C., and Rey, F.: Soil reinforcement by the roots of six dominant species on eroded mountainous marly slopes (Southern Alps, France), Catena, 84, 70–78, doi:10.1016/j.catena.2010.09.007, 2011.

Cammeraat, E., van Beek, R., and Kooijman, A.: Vegetation succession and its consequences for slope stability in SE Spain, Plant Soil, 278, 135–147, doi:10.1007/s11104-005-5893-1, 2005.

Camporeale, C., Perucca, E., Ridolfi, L., and Gurnell, A. M.: Modeling the interactions between river morphodynamics and riparian vegetation, Rev. Geophys, 51, 379–414, doi:10.1002/rog.20014, 2013.

Church, M.: Bed material transport and the morphology of alluvial river channels, Annu. Rev. Earth Pl. Sc., 34, 325–354, doi:10.1146/annurev.earth.33.092203.122721, 2006.

Clevers, J. G. P. W.: The derivation of a simplified reflectance model for the estimation of leaf area index, Remote Sens. Environ., 25, 53–69, 1988.

Copeland, R. R., McComas, D. N., Thorne, C. R., Soar, P. J., Jonas, M. M., and Fripp, J. B.: Hydraulic Design of Stream Restoration Projects, Tech. rep., US Army Corps of Engineers, Washington DC, 2001.

Croke, J., Todd, P., Thompson, C., Watson, F., Denham, R., and Khanal, G.: The use of multi temporal LiDAR to assess basin-scale erosion and deposition following the catastrophic January 2011 Lockyer flood, SE Queensland, Australia, Geomorphology, 184, 111–126, doi:10.1016/j.geomorph.2012.11.023, 2013.

Eekhout, J. P. C.: Morphological Processes in Lowland Streams. Implications for Stream Restoration, Ph.D. thesis, Wageningen University, the Netherlands, 178 pp., 2014.

Eekhout, J. P. C., Hoitink, A. J. F., and Mosselman, E.: Field experiment on alternate bar development in a straight sand-bed stream, Water Resour. Res., 49, 8357–8369, doi:10.1002/2013WR014259, 2013.

Erwin, S. O., Schmidt, J. C., Wheaton, J. M., and Wilcock, P. R.: Closing a sediment budget for a reconfigured reach of the Provo River, Utah, United States, Water Resour. Res., 48, W10512, doi:10.1029/2011WR011035, 2012.

Fattet, M., Fu, Y., Ghestem, M., Ma, W., Foulonneau, M., Nespoulous, J., Le Bissonnais, Y., and Stokes, A.: Effects of vegetation type on soil resistance to erosion: Relationship between aggregate stability and shear strength, Catena, 87, 60–69, doi:10.1016/j.catena.2011.05.006, 2011.

Fuller, I. C., Large, A. R. G., and Milan, D. J.: Quantifying channel development and sediment transfer following chute cutoff in a wandering gravel-bed river, Geomorphology, 54, 307–323, doi:10.1016/S0169-555X(02)00374-4, 2003.

Gautier, E., Brunstain, D., Vauchel, P., Jouanneau, J., Roulet, M., Garcia, C., Guyol, J., and Castro, M.: Channel and floodplain sediment dynamics in a reach of the tropical meandering Rio Beni (Bolivian Amazonia), Earth Surf. Proc. Land., 35, 1838–1853, doi:10.1002/esp.2065, 2010.

Gran, K. and Paola, C.: Riparian vegetation controls on braided stream dynamics, Water Resour. Res., 37, 3275–3284, doi:10.1029/2000WR000203, 2001.

Grove, J., Croke, J., and Thompson, C.: Quantifying different riverbank erosion processes during an extreme flood event, Earth Surf. Proc. Land., 38, 1393–1406, doi:10.1002/esp.3386, 2013.

Gurnell, A. M., Morrissey, I. P., Boitsidis, A. J., Bark, T., Clifford, N. J., Petts, G. E., and Thompson, K.: Initial Adjustments Within a New River Channel: Interactions Between Fluvial Processes, Colonizing Vegetation, and Bank Profile Development, Environ. Manage., 38, 580–596, doi:10.1007/s00267-005-0190-6, 2006.

Heritage, G. L., Milan, D. J., Large, A. R. G., and Fuller, I. C.: Influence of survey strategy and interpolation model on DEM quality, Geomorphology, 112, 334–344, doi:10.1016/j.geomorph.2009.06.024, 2009.

Holben, B. N.: Characteristics of maximum-value composite images from temporal AVHRR data, Int. J. Remote Sens., 7, 1417–1434, doi:10.1080/01431168608948945, 1986.

Kasvi, E., Vaaja, M., Alho, P., Hyyppä, J., Kaartinen, H., and Kukko, A.: Morphological changes on meander point bars associated with flow structure at different discharges, Earth Surf. Proc. Land., 38, 577–590, doi:10.1002/esp.3303, 2013.

Kleinhans, M. G.: Sorting out river channel patterns, Prog. Phys. Geog., 34, 287–326, doi:10.1177/0309133310365300, 2010.

KNMI: Langjarige gemiddelden en extremen, tijdvak 1971–2000, http://www.knmi.nl/klimatologie/normalen1971-2000/index.html (last access: 26 January 2014), 2014.

Lane, S. N., Westaway, R. M., and Hicks, D. M.: Estimation of erosion and deposition volumes in a large, gravel-bed, braided river using synoptic remote sensing, Earth Surf. Proc. Land., 28, 249–271, doi:10.1002/esp.483, 2003.

Lane, S. N., Widdison, P. E., Thomas, R. E. ans Ashworth, P. J., Best, J. L., Lunt, I. A., Sambrook Smith, G. H., and Simpson, C. J.: Quantification of braided river channel change using archival digital image analysis, Earth Surf. Proc. Land., 35, 971–985, doi:10.1002/esp.2015, 2010.

Legleiter, C. J. and Kyriakidis, P. C.: Forward and inverse transformations between cartesian and channel-fitted coordinate systems for meandering rivers, Math. Geol., 38, 927–958, doi:10.1007/s11004-006-9056-6, 2007.

Lejot, J., Delacourt, C., Piégay, H., Fournier, T., Trémélo, M.-L., and Allemand, P.: Very high spatial resolution imagery for channel bathymetry and topography from an unmanned mapping controlled platform, Earth Surf. Proc. Land., 32, 1705–1725, doi:10.1002/esp.1595, 2007.

Leopold, L. B. and Bull, W. B.: Base level, aggradation, and grade, P. Am. Philos. Soc., 123, 168–202, 1979.

Mackin, J. H.: Concept of the Graded River, Geol. Soc. Am. Bull., 59, 463–512, doi:10.1130/0016-7606(1948)59[463:COTGR]2.0.CO;2, 1948.

Milan, D. J., Heritage, G. L., Large, A. R. G., and Fuller, I. C.: Filtering spatial error from DEMs: Implications for morphological change estimation, Geomorphology, 125, 160–171, doi:10.1016/j.geomorph.2010.09.012, 2011.

Perucca, E., Camporeale, C., and Ridolfi, L.: Significance of the riparian vegetation dynamics on meandering river morphodynamics, Water Resour. Res., 43, W03430, doi:10.1029/2006WR005234, 2007.

Pollen-Bankhead, N. and Simon, A.: Enhanced application of root-reinforcement algorithms for bank-stability modeling, Earth Surf. Proc. Land., 34, 471–480, doi:10.1002/esp.1690, 2009.

Rosgen, D. L.: A classification of natural rivers, Catena, 22, 169–199, 1994.

Shields, F. D., Copeland, R. R., Klingeman, P. C., Doyle, M. W., and Simon, A.: Design for stream restoration, J. Hydraul. Eng. ASCE, 129, 575–584, doi:10.1061/(ASCE)0733-9429(2003)129:8(575), 2003.

Simon, A. and Collison, A. J. C.: Quantifying the mechanical and hydrologic effects of riparian vegetation on streambank stability, Earth Surf. Proc. Land., 27, 527–546, doi:10.1002/esp.325, 2002.

Tal, M. and Paola, C.: Dynamic single-thread channels maintained by the interaction of flow and vegetation, Geology, 35, 347–350, doi:10.1130/G23260A.1, 2007.

Tal, M. and Paola, C.: Effects of vegetation on channel morphodynamics: Results and insights from laboratory experiments, Earth Surf. Proc. Land., 35, 1014–1028, doi:10.1002/esp.1908, 2010.

Van de Wiel, M. J. and Darby, S. E.: Riparian Vegetation and Fluvial Geomorphology, chap. Numerical modeling of bed topography and bank erosion along tree-lined meandering rivers, pp. 267–282, Water Science and Application Series 8, American Geophysical Union, Washington, DC, 2004.

Van Heerd, R. M., Kuijlaars, E. A. C., Teeuw, M. P., and Van 't Zand, R. J.: Productspecificatie AHN 2000, Tech. Rep. MDTGM 2000.13, Rijkswaterstaat, Adviesdienst Geo-informatie en ICT, Delft, 2000.

Wheaton, J. M., Brasington, J., Darby, S. E., Merz, J., Pasternack, G. B., Sear, D., and Vericat, D.: Linking geomorphic changes to salmond habitat at a scale relevant to fish, River Res. Appl., 26, 469–486, doi:10.1002/rra.1305, 2010a.

Wheaton, J. M., Brasington, J., Darby, S. E., and Sear, D. A.: Accounting for uncertainty in DEMs from repeat topographic surveys: Improved sediment budgets, Earth Surf. Proc. Land., 35, 136–156, doi:10.1002/esp.1886, 2010b.

Wheaton, J. M., Brasington, J., Darby, S. E., Kasprak, A., Sear, D., and Vericat, D.: Morphodynamic signatures of braiding mechanisms as expressed through change in sediment storage in a gravel-bed river, J. Geophys. Res., 118, 759–779, doi:10.1002/jgrf.20060, 2013.

Wilkerson, G. V. and Parker, G.: Physical basis for quasi-universal relationships describing bankfull hydraulic geometry of sand-bed rivers, J. Hydraul. Eng. ASCE, 137, 739–753, doi:10.1061/(ASCE)HY.1943-7900.0000352, 2011.

Wynn, T. M., Mostaghimi, S., Burger, J. A., Harpold, A. A., Henderson, M. B., and Henry, L. A.: Variation in Root Density along Stream Banks, J. Environ. Qual., 33, 2030–2039, 2004.